

^{139}La NQR relaxation and μSR study of Zn-doping effects in La_2CuO_4

M. Corti, A. Rigamonti, and F. Tabak*

Department of Physics "A. Volta" and Unità INFN, University of Pavia, Via Bassi 6, I-27100 Pavia, Italy

P. Carretta

LCMI-MPI, CNRS, 25 Av. des Martyrs, 38042 Grenoble, France

F. Licci and L. Raffo

Istituto MASPEC (CNR), 43100 Parma, Italy

(Received 13 February 1995)

^{139}La NQR and zero-field $\mu^+\text{SR}$ in antiferromagnetic (AF) $\text{La}_2\text{Cu}_{1-x}\text{Zn}_x\text{O}_4$, for x up to 0.13 and in the temperature range 1.6–350 K, are used to study the effects related to the substitution of magnetic Cu^{2+} $S = \frac{1}{2}$ with homovalent diamagnetic $S = 0$ Zn^{2+} in La_2CuO_4 . We report measurements both of static magnetic properties, such as Néel temperatures T_N , sublattice magnetization and field $|\mathbf{h}|$ at the La nucleus or at the μ^+ site, as well as of NQR relaxation rates W . These quantities are used to study the effects of Zn doping on the low-energy Cu^{2+} spin excitations. It is found that T_N decreases with x in a way close to the one expected by diluting quasi-two-dimensional Heisenberg magnets on square lattice, while the sublattice magnetization is slightly affected by Zn doping. Mean-field arguments based on the dilution model for the interplanar interactions allow one to conclude that the in-plane magnetic correlation length is little sensitive to the Zn presence. Up to $x \approx 0.08$ the temperature dependence of the AF field $|\mathbf{h}|$ is close to the one in pure La_2CuO_4 , with a sharp decrease for $T \rightarrow T_N^-$ indicative of a continuous transition with a small critical exponent β . For strong doping the low-temperature dependence of $|\mathbf{h}|$ appears to depart from the one in pure La_2CuO_4 . For $x \geq 0.05$ both NQR spectra and μSR reveal the presence of regions where the long-range AF order is suppressed. For temperature above 100 K up to T_N the ^{139}La relaxation rate W due to the Cu^{2+} spin fluctuations shows only slight corrections with respect to pure La_2CuO_4 which are possibly related to the disorder in the AF interactions or to finite-size effects. A novel and remarkable effect of Zn doping is the appearance in W , for $T \leq 100$ K, of large and marked maxima, which are x dependent. This phenomenon is attributed to the cooperative freezing of local magnetic moments induced by Zn on Cu orbitals, interacting via the underlying AF matrix. The maxima in W occur when the fluctuation frequencies of the anomalous spins become of the order of the NQR frequency, thus driving the system to a spin-glass state superimposed to the AF matrix.

I. INTRODUCTION

The study of the effects of Zn for Cu substitution in La_2CuO_4 is motivated both by the growing interest in the quantum magnetism of this $S = \frac{1}{2}$ quasi-two-dimensional (2D) Heisenberg antiferromagnet (AF), as well as by the connections with the mechanism of superconductivity in cuprates, known to occur on the verge of the AF order.¹ The additional electron introduced by replacing Cu^{2+} by $S = 0$ Zn^{2+} is tightly bound to the donor site and thus in $\text{La}_2\text{Cu}_{1-x}\text{Zn}_x\text{O}_4$ one has a removal of a $S = \frac{1}{2}$ Cu^{2+} spin from the AF matrix. This situation is somewhat equivalent to the spin vacancy induced by Sr doping, the relevant difference being that in $\text{La}_{2-x}\text{Sr}_x\text{CuO}_4$ the spin vacancy is itinerant. Only for low temperature and light x can localization occur, with modification in the AF spin texture.^{2,3}

In nominally pure La_2CuO_4 , the Néel temperature T_N is around 315 K, while extra oxygen defects decrease it. Charge defects (and therefore also oxygen deficiencies possibly compensated by La deficiency) drastically affect T_N . The interplay of Zn for Cu substitution with the simultaneous change in the oxygen stoichiometry led to

the conclusion⁴ that Zn doping affects the magnetic properties of La_2CuO_4 in a way stronger than the conventional magnetic dilution. Theoretical treatments⁵ for a 2D Heisenberg AF on a square lattice, supported by experimental results in the compounds of the K_2NiF_4 family,⁶ indicate for the initial suppression rate

$$A = -\frac{1}{T_N} \lim_{x \rightarrow 0} \frac{dT_N(x)}{dx}, \quad (1)$$

a value around π , with a percolation threshold $x \approx 0.41$ for the AF order. When the oxygen content is kept unaffected, susceptibility measurements⁷ showed that A is actually around 4 while the percolation threshold is above $x = 0.2$. The effective Cu magnetic moment^{6,7} is almost insensitive to changes in x . On the other hand, Zn doping dramatically reduces the superconducting transition temperature in $\text{La}_{2-x}\text{Sr}_x\text{CuO}_4$ and in $\text{YBa}_2\text{Cu}_3\text{O}_{7-\delta}$.⁸ Furthermore, Zn for Cu substitution in $\text{YBa}_2\text{Cu}_3\text{O}_{6+x}$ induces local magnetic moments on Cu orbitals, as deduced from ^{89}Y NMR (Ref. 9) and μSR (Ref. 10). Thus one is led to the conclusion that novel microscopic features such as effects on the electronic states, not included in magnetic dilution models, occur in

$\text{La}_2\text{Cu}_{1-x}\text{Zn}_x\text{O}_4$. Finally, it should be mentioned that the dynamical properties, involving spin fluctuations and correlated spin dynamics, are largely unexplored in this compound.

^{139}La nuclear quadrupole resonance (NQR) and spin-lattice relaxation have proved useful tools to study the microscopic static and dynamical properties in charge-doped La_2CuO_4 . A variety of experiments¹¹ have provided enlightening insights in $\text{La}_{2-x}\text{Sr}_x\text{CuO}_4$.

In this paper we report the results of ^{139}La NQR spectra and relaxation rates and of μSR precessional frequencies on $\text{La}_2\text{Cu}_{1-x}\text{Zn}_x\text{O}_4$, for Zn doping up to 13% and in the temperature range 1.6–350 K. The analysis of the experimental findings allows us to derive static quantities, such as the Néel temperature, Cu sublattice magnetization and the x and temperature dependence of the magnetic field $|\mathbf{h}|$. The ^{139}La relaxation rates are used to derive information on the Cu^{2+} spin dynamics in the AF phases. In particular, the effect of Zn in generating local magnetic moments is addressed, showing that their cooperative freezing drives the system in a spin-glass phase. Quantitative information on the decay rates of the spin fluctuations and on their x and temperature dependences are thus obtained. Comparison with the situation occurring in La_2CuO_4 upon charge doping is also made, in particular with regard to the spin-glass state arising upon charge localization.³ Preliminary and partial results of our study have already been reported in meetings.¹²

The paper is organized as follows. In Sec. II details on the experimental aspects will be given. In Sec. III the results for static quantities, i.e., magnetization, field, and Néel temperature through NQR spectra and $\mu^+\text{SR}$ precessional frequencies are presented, followed by the ^{139}La NQR relaxation rates driven by the time-dependent part of the hyperfine magnetic interaction of La nuclei with the Cu^{2+} electronic spins. Section IV is devoted to a thorough analysis, in particular with regard to the Zn effects on the in-plane magnetic correlation length and to the x and temperature dependences of the fluctuation frequencies of the magnetic moments induced by Zn doping, vis-à-vis to the correspondent effects resulting from the charge localization in Sr-doped La_2CuO_4 .

II. EXPERIMENT

A. Sample preparation

The Zn-doped La_2CuO_4 and pure La_2CuO_4 used as a reference were prepared by conventional solid-state reaction in air, with annealing of the pellets for 24–48 h at 1050 °C. The treatment was repeated 3 or 4 times with intermediate cooling and accurate grinding. Annealing at 480–500 °C in oxygen was first performed for 150–200 h in order to fully oxidize the products.

Particular attention has been devoted to the role of extra oxygen, which is known⁷ to cause a depression of T_N stronger than the one due to Zn, particularly in Zn-doped $\text{YBa}_2\text{Cu}_3\text{O}_{7-\delta}$ (Refs. 13 and 14). NQR measurements were first carried out in as-grown samples. Then a set of samples was kept for 24 h at various temperatures from 600 to 900 °C in N_2 atmosphere. T_N was found to in-

crease progressively, supporting the conclusion¹⁵ that the effect of interstitial oxygen simply adds to the one of the magnetic vacancies due to Zn. In the thermally treated samples, thermogravimetric measurements did not detect extra oxygen. For $x=0$ we found $T_N \simeq 315 \pm 2$ K, close to the highest T_N 's achieved in La_2CuO_4 ceramics. In another batch of samples used for $\mu^+\text{SR}$, the interstitial oxygen was removed by sealing in evacuated ampoules in the presence of metallic zirconium and then treated at 450 °C for 120 h (Ref. 16). The Néel temperature indicated by the extrapolation of the μSR precessional frequencies in pure La_2CuO_4 turned out to be $T_N = 312 \pm 5$ K. Some evidence of small amounts of extra oxygen was still noticed from the contribution to ^{139}La NQR relaxation in the high-temperature ($T \geq 300$ K) region. The NQR relaxation is very sensitive to the diffusion of intercalated oxygen.¹⁷ According to the sensitivity of thermogravimetric measurements, the oxygen possibly still present is less than one part over 10^3 . In view of the above consideration on the addition effect and of the small amount of oxygen, if any, we believe that the main conclusions derived in the following are not affected by the oxygen stoichiometry. In this respect, one should remark that the Néel temperatures in our samples are practically coincident with the ones from Cheong *et al.*,⁷ where emphasis on the proper oxygen content was kept (see below).

B. NQR spectra

The ^{139}La NQR spectra have been obtained with a variable-power pulse FT spectrometer (Bruker MSL 200) with different techniques, depending on the linewidth. For relatively narrow lines, as in pure or lightly doped La_2CuO_4 [full width half intensity (FWHI) $\Delta \leq 100$ kHz], the spectra were obtained by direct Fourier transformation (FT) of half of the echo signal following the usual $(\pi/2 - \pi)$ -like sequence of high-power rf pulses. For broad lines, as the ones in strongly doped samples, the spectra have been derived from the echo envelope by sweeping the irradiation frequency ν_{irr} at moderate intensity of the rf field. Also the FT of the echo obtained at different ν_{irr} was performed in the same cases and the spectra reconstructed from the amplitude of the signal read at ν_{irr} .

The NQR spectra have been used to derive the internal field $|\mathbf{h}(x, T)|$ at the La site, in the AF phases. For $T \rightarrow 0$, the ratio $|\mathbf{h}(x, 0)|/|\mathbf{h}(0, 0)|$ directly yields the reduction of the Cu sublattice magnetization to which the field is proportional, in the assumption that no modifications in the AF magnetic structure or in the electric-field (EFG) occur on doping.

The field at the La site was obtained from the lines originated from the mixed eigenstates of the $\pm \frac{1}{2} \leftrightarrow \pm \frac{3}{2}$ levels.¹⁸ In particular, the shift δ of the doublet at higher frequency with respect to the quadrupole frequency $\nu_Q = e^2qQ/4h$ was measured [see Fig. 1(a)]. The field $|\mathbf{h}(x, T)|$ was then derived from $\delta(x, T)$ through diagonalization of the matrix for the Zeeman-perturbed quadrupole levels, in correspondence to the best-fit values for ν_Q and for the asymmetry parameter η of the EFG. For pure La_2CuO_4 , the field and the EFG parameters

$[|\mathbf{h}(0,0)|=997\pm 10$ G, angle θ between \mathbf{h} and V_{zz} , $\theta=78^\circ\pm 0.5^\circ$, $\eta\simeq 0.01$, and $\nu_Q=6.38$ MHz] are in good agreement with previous results.^{18,19} It should be noted that δ is practically linear in $|\mathbf{h}|$ only for $|\mathbf{h}|\geq 700$ G (and then $T\rightarrow 0$). For $(T/T_N)\geq 0.5$, namely, $|\mathbf{h}|\leq 600$ G, one has approximately δ (MHz) $=|\mathbf{h}$ (kG)^{0.8}. While in pure La_2CuO_4 the NQR lines are rather narrow (FWHM $\Delta\simeq 70$ kHz; see the subsequent section), upon Zn doping a marked broadening is observed [Fig. 1(b)]. The broadening is of quadrupolar origin (distribution of EFG's, stresses, etc.) and/or related to static disorder in the staggered magnetization. It appears similar to one observed upon Sr for La substitution.¹¹ The related decrease in resolution causes a larger error in the estimate of the field for large x , particularly close to T_N . This difficulty is

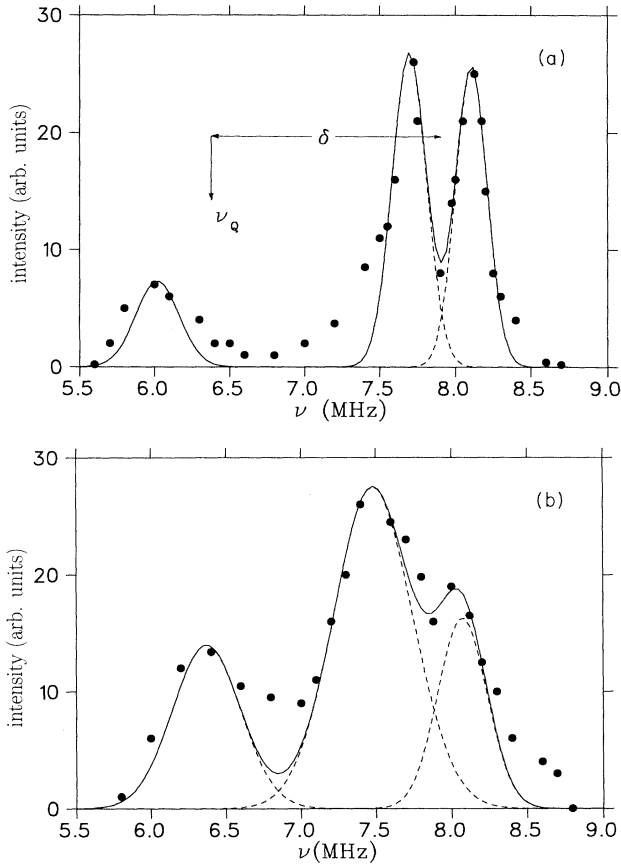


FIG. 1. Typical ^{139}La NQR low-frequency (mixed Zeeman quadrupole eigenstates $\pm\frac{1}{2}\leftrightarrow\pm\frac{3}{2}$) spectra in $\text{La}_2\text{Cu}_{1-x}\text{Zn}_x\text{O}_4$. (a) shows the case for $x=0.025$ ($T\simeq 4.2$ K), where the broadening of the lines with respect to pure La_2CuO_4 is moderate (about a factor of 2) and the line at $\nu_Q=6.38$ MHz (correspondent to one-third of the doublet at $\approx 3\nu_Q$) is absent. (b) refers to $x=0.11$ and evidences the marked broadening of the lines (dotted lines) yielding the spectrum. Furthermore, in this case a line at frequency $\approx\nu_Q$, corresponding to “paramagnetic” regions of the sample where $|\mathbf{h}|=0$ (see text) is already present at $T\simeq 11$ K. The line at $\nu\simeq 5.9$ MHz in (a) is the other component originated from the $(\pm\frac{1}{2}\leftrightarrow\pm\frac{3}{2})$ Zeeman perturbed quadrupolar eigenstates and it is poorly reproduced because of the decrease in sensitivity of our receiver below 6 MHz.

present to a smaller extent in the evaluation of $|\mathbf{h}|$ through μSR . Finally, it is worth mentioning that the distribution of the EFG's associated with the Zn impurity in principle could be strong enough that NQR signals from the nuclei nearby are missed. A comparison of the area of the signals for $x=0$ and $x=0.05$ indicated that most of the La nuclei, including the nearest neighbors to the impurity, were actually irradiated, their NQR frequency being changed within the linewidth.

C. Zero-field (ZF) μ^+ SR

ZF μ^+ SR measurements have been carried out at Rutherford Appleton Laboratory on a beamline with 100% spin-polarized 29 MeV/c muons. The time evolution of muon polarization was detected over 16 μs . The spurious signal due to the cryostat walls and silver shieldings was previously calibrated by replacing the sample with natural hematite. The decay of the polarization of μ^+ stopped in the sample was fitted according to the relation

$$P_\mu(t) = A_1 e^{-\sigma t} \cos(\gamma B_\mu t + \phi) + A_2 e^{-\lambda t}, \quad (2)$$

$\gamma=2\pi 135.5$ MHz/T being the muon gyromagnetic ratio, B_μ the local field at the muon, and σ and λ the transverse and longitudinal decay rates, respectively. The two components originate from muons in grains where \mathbf{B}_μ is transverse or parallel to the beam polarization. The ratio A_1/A_2 differs from the purely geometrical value $(A_1/A_2)=2$ because of the different filtering effects related to the muon pulse duration (72 ns). Thus (A_1/A_2) is also a function of temperature in view of that of the precessional frequencies.

Below $T\simeq 100$ K, in some samples, a small fraction of muons was detected to precess around a field $B_\mu\simeq 100$ G. This fraction is possible associated to μ^+ stopped near oxygen vacancies, their localization becoming stable only at low temperatures. On the other hand, in a restricted temperature range below T_N , a distinct fraction of muons in zero field was detected (see Sec. III A).

D. ^{139}La NQR relaxation rates

The ^{139}La NQR relaxation rates W have been derived from the recovery of the echo amplitude $s(t)$ due to the $(\pm\frac{5}{2}\leftrightarrow\pm\frac{7}{2})$ line after saturation. The recovery law $y(t)=[s(\infty)-s(t)]/s(\infty)$ is related to W in a way depending on the relaxation mechanism (quadrupolar, namely, due to the time-dependent part of the EFG's or magnetic, i.e., driven by the fluctuations in the effective magnetic field at the La site). In the AF phases, with the possible exclusion of the high-temperature range in pure La_2CuO_4 , the relaxation mechanism is mostly magnetic, as it turns out from a comparison of the recovery laws for the $\approx 2\nu_Q$ and $\approx 3\nu_Q$ lines under different irradiation condition.²⁰ In particular, the magnetic mechanism is dominant in the temperature range below 100 K in view of the fast decrease, on cooling, of the quadrupolar two-phonon Raman relaxation process (in the low-temperature range the quadrupolar relaxation rate goes as¹¹ $W\propto T^7$).

For the magnetic relaxation mechanism and fast saturation of the $\pm\frac{5}{2} \leftrightarrow \pm\frac{7}{2}$ line, from the solution of the master equations for the populations of the NQR levels, one obtains for the recovery law^{11,20,21}

$$y(t) = 0.746e^{-20Wt} + 0.071e^{-6Wt} + 0.181e^{-42Wt}. \quad (3)$$

For $T \geq 100$ K and $T \leq 20$ K this recovery law fitted well the experimental results and the spin-lattice relaxation rate $2W$ was thus directly obtained. It can be mentioned that the removal of the $\pm m$ degeneracy due to static field²¹ has practically no effect in Zn-doped La_2CuO_4 in view of the quadrupolar broadening of the levels. For broad lines, in order to grant the initial condition of full saturation, a sequence of five to ten rf pulses lasting less than W^{-1} was used. It is noted that Eq. (3) in the first decade ($y \geq 0.1$) does not differ much from an exponential with time constant $\approx 23W$.²⁰

In the temperature range $20 \text{ K} \leq T \leq 100 \text{ K}$ and particularly for T around the temperature T_m at which $2W$ exhibit marked maxima (see the experimental results in Sec. III D), the recovery laws depart from Eq. (3) and a relation of the form

$$y(t) = e^{-(W_e t)^{1/2}} \quad (4)$$

yielded a good fit to the data (see the illustrative example in Fig. 2). The relevant implication of the changeover in the recovery law for $T \approx T_m$ will be discussed in Sec. IV.

The magnetic relaxation rate in Eqs. (3) and (4) can be written¹¹

$$2W = \frac{\gamma^2}{2} \int \langle \mathbf{h}_+(0) \mathbf{h}_-(t) \rangle e^{-i3\omega_e t} dt, \quad (5)$$

where \mathbf{h} is the fictitious magnetic field at the La site related to time dependence of the Cu^{2+} spin operator \mathbf{S} or from other sources of time-dependent magnetic nucleus-electron interaction (see Sec. IV for further details). In

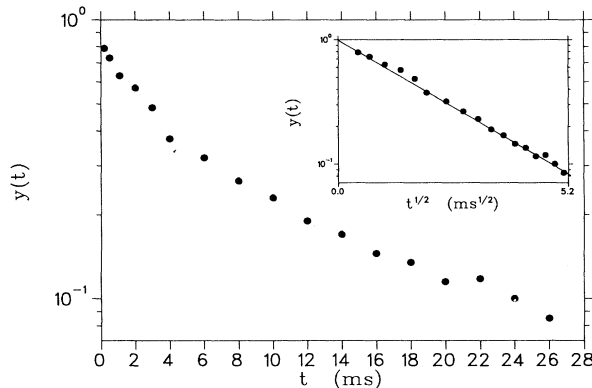


FIG. 2. Typical recovery plots $y(t) = [s(\infty) - s(t)] / s(\infty)$ of the NQR signals after saturation of the $(\pm\frac{5}{2} \leftrightarrow \pm\frac{7}{2})$ line in $\text{La}_2\text{Cu}_{1-x}\text{Zn}_x\text{O}_4$ observed around the temperature T_m at which the relaxation rates show maxima. As is shown in the inset, the recovery follows Eq. (4) in the text. On the contrary, for $T \geq 100$ K and $T \leq 20$ K, the recovery was well described by Eq. (3) in the text.

Eq. (5), the Fourier transform of the correlation function for the field components is at $3\omega_Q$, since the $\pm\frac{5}{2} \leftrightarrow \pm\frac{7}{2}$ line used for the measures of W occurs at about three times the quadrupole frequency.

Finally, we remark that the decay rate of the spin fluctuations at the muon sites cannot be obtained by measuring λ [Eq. (2)]. In fact, the value of $\lambda = 2W_\mu$ expected for muons should be of the order of $W(\gamma_\mu / \gamma_{\text{La}})^2$. For a maximum of W around 10 s^{-1} for $x = 0.08$ (see below), the contribution to λ from the Cu^{2+} spin fluctuations is too small to be detected ($\lambda_{\text{max}} \leq 5 \times 10^{-3} \mu\text{s}^{-1}$).

III. EXPERIMENTAL RESULTS

In this section the experimental results for T_N , for the sublattice magnetization $\langle \mu_{\text{Cu}} \rangle$ (average of the spin component along the local quantization axis), for the internal field, and for the relaxation rates in $\text{La}_2\text{Cu}_{1-x}\text{Zn}_x\text{O}_4$ are reported. In the perspective of the analysis of the data, a brief presentation of the results for pure La_2CuO_4 is first given.

In the paramagnetic phase of pure La_2CuO_4 ($T \geq 315$ K), the relatively narrow NQR lines (typically $\Delta \approx 70$ kHz) in our powders are an indication of the good quality of the compounds, in terms of lattice defects and/or oxygen stoichiometry. It should be noted, in fact, that only for high-quality single crystals are smaller widths observed.²² In a powder the random orientation of the V_{zz} EFG axis with respect to the rf field necessarily broadens the lines.

In Fig. 3 the temperature dependence of the field $|\mathbf{h}(0, T)|$ estimated from δ (see Sec. II B) and from the μSR precessional frequencies is shown. An apparent discontinuity for T close to T_N^- is observed, consistent with observations by other authors.²²⁻²⁴ The AF transition, purely magnetic in origin, is actually second order,²² with a continuous onset of the sublattice magnetization characterized by a small critical exponent β . An indicative value $\beta \approx 0.15$ satisfactorily fits the temperature behavior of $|\mathbf{h}|$ in Fig. 3.

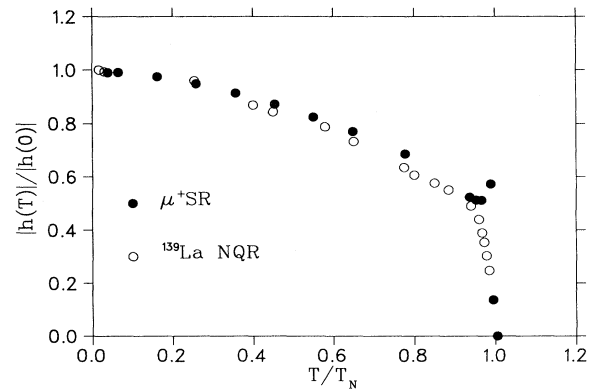


FIG. 3. Normalized temperature dependent of the field $|\mathbf{h}(T)|$ derived in undoped La_2CuO_4 from the estimate of $\delta(0)$ (see text in Sec. III) and from the muon precessional frequencies. The Néel temperature was found to be $T_N = 315 \pm 2$ K from the NQR spectra and $T_N = 312 \pm 5$ K in μSR .

Even close to T_N , no coexistence of unsplit pure NQR and Zeeman split lines, indicating both paramagnetic (PM) and AF phases, was detected in pure La_2CuO_4 .

The ^{139}La NQR spin-lattice relaxation rates in La_2CuO_4 were found to be consistent with previous measurements for almost stoichiometric samples.¹¹ A sketchy behavior of $2W$ as a function of temperature will be reported in Fig. 7 for comparison with the Zn-doped compounds.

A. Néel temperatures in $\text{La}_2\text{Cu}_{1-x}\text{Zn}_x\text{O}_4$

From NQR the Néel temperatures $T_N(x)$ have been estimated from the condition $\delta(x, T) \rightarrow 0$ in the spectra as well as from the spin-lattice and spin-spin relaxation rates which display peaks at the PM-AF transition.¹¹ In $\mu^+\text{SR}$, T_N was estimated from the extrapolation $B_\mu(T) \rightarrow 0$.

The results for $T_N(x)$ are reported in Fig. 4, by including representative data obtained by other authors with different techniques. The solid line corresponds to an initial suppression rate [Eq. (1)] $A=4$. The dash-dotted line qualitatively marks the region in which PM lines (corresponding to $|\mathbf{h}=0\rangle$) coexist with the AF ones. For $x \geq 0.05$, the PM line is present also for $T \ll T_N$ [see Fig. 1(b)]. The coexistence of PM and AF regions can be attributed to a kind of microscopic phase separation in Zn-rich and Zn-depleted phases.

The paramagnetic regions are also evidenced in μSR as the fraction of muons in zero field. In particular, for $x=0.08$ this fraction increases progressively on heating towards T_N , in a way similar to Sr-doped La_2CuO_4 .²⁶ Coexistence of ordered AF regions and of short-length

disordered phases was first noticed in $\text{La}_2\text{Cu}_{1-x}\text{Zn}_x\text{O}_4$ from $\mu^+\text{SR}$ by Lichti *et al.*²⁷ Their Néel temperatures (not reported in Fig. 4) drop with x faster than ours, analogous to the data reported by Ting *et al.*²⁸ The presence in their samples of extrastochiometric oxygen can be suspected in view of the low T_N (≈ 250 K) in their pure La_2CuO_4 .

Finally, we remark that the magnetization measurements by Zysler *et al.*²⁵ (data reported in Fig. 4) on samples from the same batch, yielding $T_N(x)$ slightly lower than ours, could reflect the presence of Zn-rich phases, for $x \geq 0.05$.

B. Sublattice magnetization

From the comparison of the NQR spectra and $\mu^+\text{SR}$ frequencies at the lowest temperatures with the ones in pure La_2CuO_4 , the x dependence of the sublattice magnetization can be directly obtained. In fact, no change in the magnetic lattice upon Zn doping should occur, at least for $x \leq 0.08$. The temperature behavior of the field is actually smooth and strictly similar to the one in pure La_2CuO_4 (see Sec. III C).

The sublattice magnetization (Fig. 5) is slightly sensitive to Zn doping, consistent with previous observations, although not entirely unaffected. The initial suppression rate $B = -\lim_{x \rightarrow 0} (d/dx)[\mu(x)/\mu(0)]$ is close to 1. It should be remarked that for $x=0.11$ and 0.13 the estimate of $\langle \mu_{\text{Cu}} \rangle$ can be affected by changes in the magnetic structure (see the following subsection).

C. Temperature dependence of the AF field

Through the evaluation of $\delta(x, T)$ in the NQR spectra and from the μ^+ precessional frequencies, the temperature dependence of the internal field at the La nuclei and at the muons can be obtained. From Fig. 6 it may be noted that for $x=0.075$ the values for $|\mathbf{h}|$ deduced from the NQR spectra are affected by some uncertainty, in view of the broadening of the lines. The values for

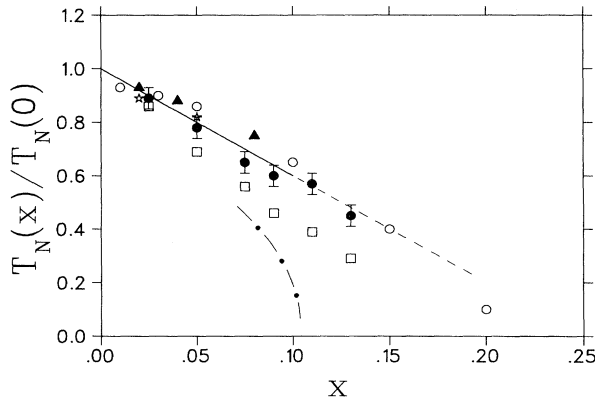


FIG. 4. x dependence of the Néel temperatures T_N in $\text{La}_2\text{Cu}_{1-x}\text{Zn}_x\text{O}_4$ (normalized to the one in pure La_2CuO_4) as derived from the NQR measurements (●) and from $\mu^+\text{SR}$ precessional frequency (▲). Results from other authors which appear reliable (absence of extrastochiometric oxygen) have also been reported for comparison: (○), Cheong *et al.*, Ref. 7 and (☆), Keimer *et al.*, Ref. 15. The squares (□) refer to magnetization measurements from Zysler *et al.* (Ref. 25) on samples of the same batch. The solid line corresponds to an initial suppression rate [Eq. (1)] $A=4$. The dash-dotted line indicates that for $x \geq 0.05$, a “paramagnetic” phase (namely, $T_N \rightarrow 0$), corresponding to zero static field, was found both in the NQR spectra [see Fig. 1(b)] as well as in μSR for $T \rightarrow T_N^{-1}$ (see text).

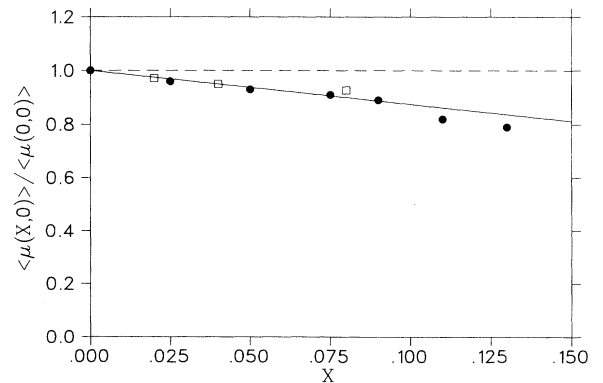


FIG. 5. x dependence of the sublattice magnetization $\langle \mu(x, T \rightarrow 0) \rangle$ (average of the Cu^{2+} magnetic moment along a local quantization axis) in $\text{La}_2\text{Cu}_{1-x}\text{Zn}_x\text{O}_4$, as obtained from the comparison of the NQR spectra (●) and μSR precessional frequencies (□) with the correspondent ones in pure La_2CuO_4 .

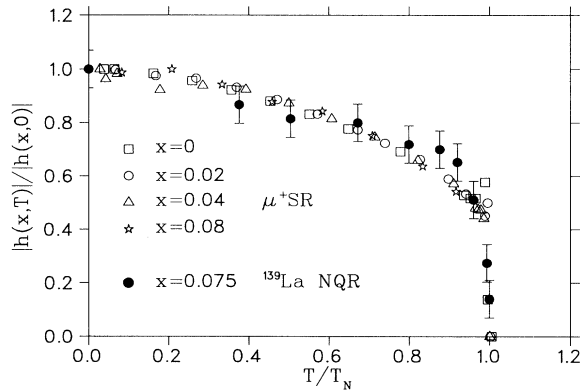


FIG. 6. Normalized temperature dependence of the internal field $|\mathbf{h}(x,T)|$ as obtained from the comparison of the $\mu^+\text{SR}$ precessional frequencies and ^{139}La NQR spectra with the ones at the lowest temperatures, as a function of $T/T_N(x)$ (see Fig. 4). For NQR we show only the data for $x=0.075$, the doping amount for which a departure from the smooth behavior indicated by $\mu^+\text{SR}$ begins to be noticeable. Typical errors are indicated in this case.

$|\mathbf{h}(x,T)|/|\mathbf{h}(x,0)|$ extracted from the broad NQR lines for $x=0.11$ and 0.13 are characterized by a large error. It seems possible, however, to conclude that the behavior of the field for large x departs from the one for $x \leq 0.08$ shown in Fig. 6. In particular, a sudden reduction of $|\mathbf{h}|$ in the temperature range $0 \leq T \leq 0.2T_N$ is observed, similar to the one detected^{26,29} in Sr-doped La_2CuO_4 . For $x=0.11$ and 0.13 also the apparent Cu^{2+} magnetic moment shows a departure from the linear decrease with x (see Fig. 5). Thus, it can be suspected that for strong Zn doping modifications in the magnetic lattice actually occur. The poor resolution and the simultaneous presence of the PM regions prevent a quantitative analysis of the static magnetic effects for large Zn doping. Further work with improved NQR resolution and comparison with $\mu^+\text{SR}$ would be necessary in order to investigate the modification of the static AF field for strong ($x \geq 0.1$) doping.

On the contrary, the dynamical effects associated to extramagnetic moments induced by Zn doping on the AF matrix are evident from the La NQR relaxation rates, as we will see in the following.

D. ^{139}La NQR relaxation rates

In Fig. 7 the ^{139}La relaxation rates $2W$ extracted from the recovery plots as described in Sec. IID are shown. For the sample at $x=0.025$, the measurements before and after the thermal treatment prove that the broad maximum $2W$ for $T \approx 40$ K is not due to extra oxygen. In fact, in the samples at $x=0.025$ and 0.075 , the relaxation rate below about 100 K did not change during the thermal treatment, although the removal of the oxygen increased the Néel temperature. It should be reminded that for $T \geq 100$ K and $T \leq 20$ K the recovery plots are well fitted by Eq. (3). On the contrary for $T \approx T_m$, the recovery is described by Eq. (4) (Fig. 2).

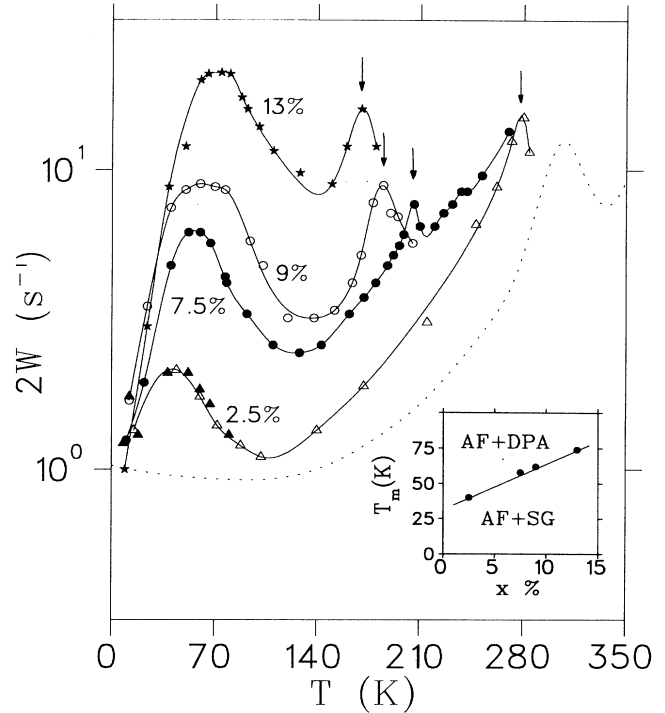


FIG. 7. Semilog plots of the temperature dependence of the ^{139}La NQR relaxation rate $2W$ in the AF phases of $\text{La}_2\text{Cu}_{1-x}\text{Zn}_x\text{O}_4$ for $x=0.025$ ($\blacktriangle, \triangle$ before and after the thermal treatment in N_2 atmosphere to remove the extra oxygen) for $x=0.075$ (\bullet), for $x=0.09$ (\circ), and for $x=0.13$ (\star). The dotted line is the sketchy behavior for pure La_2CuO_4 . The arrows mark the Néel temperatures, as deduced from the condition $\delta(x,T) \rightarrow 0$ and from the peaks in the spin-spin and spin-lattice relaxation rates. For $T \approx T_m$, where the relaxation rates have their maxima and the recovery laws change from Eq. (3) to Eq. (4), we have reported in the figure the quantities $2W_e = (T_{1e})^{-1}/11.5$, where T_{1e} is the time constant at which y is reduced to $1/e$. The inset shows the phase diagram, with a disordered paramagnet in the AF matrix above $T_g \equiv T_m$ (see text) and a spin-glass state below.

IV. ANALYSIS OF THE RESULTS AND DISCUSSION

We first discuss the results regarding the sublattice magnetizations and the Néel temperatures. Recent findings in the AF phases of $\text{La}_2\text{Cu}_{1-x}\text{Zn}_x\text{O}_4$ (Refs. 4,7,27) and of $\text{YBa}_2\text{Cu}_{3-x}\text{Zn}_x\text{O}_6$ (Ref. 30) with different techniques indicated that the sublattice magnetization is unaffected by Zn doping. Our data (Fig. 5) show that the Cu magnetic moment is almost insensitive to changes in x , to an extent compatible with the dilution model. The suppression rate A for $T_N(x)$ (Fig. 4) is larger than the one for $\langle \mu_{\text{Cu}} \rangle$, although not far from the theoretical value for Heisenberg (H) AF on a 2D square lattice.⁵ The lack of a deep theoretical understanding of magnetic dilution effects in quantum 2D H systems discourages quantitative analysis. In light of recent theoretical developments,^{31,32} specifically for La_2CuO_4 , the x dependence of T_N can tentatively be discussed in terms of modification in the magnetic correlation length ξ . By including the substitutional effect on the interplanar interaction $J_1(x)$

within the dilution model, the 3D ordering temperature for H 2D AF can be written³¹

$$T_N = \frac{J_{\perp}(0)}{k} (1-x)^2 \xi_{2D}^2(x, T_N). \quad (6)$$

The in-plane correlation length ξ_{2D} (in lattice unit a) is given by^{33,34}

$$\xi_{2D} = \frac{e\hbar c_{sw}}{16\pi a k T_s} \left[1 - \frac{1}{2} \frac{T}{2\pi T_s} \right] e^{2\pi T_s/T}, \quad (7)$$

where c_{sw} is the spin-wave velocity, T_s the spin stiffness $T_s = c_{sw}^2 \chi_{\perp}/k$ (χ_{\perp} zero-temperature transverse susceptibility), and $2\pi T_s \simeq 1.13 T_{exch}$, with $T_{exch} = J_{exch}/k$.

Zn doping can be expected to affect T_N because of the reduction of ξ_{2D} caused by the decrease of the spin stiffness T_s .³¹ In the low concentration limit, for a square lattice one derives³⁵

$$T_s(x) \simeq T_s(0) [1 - (2-x)x]. \quad (8)$$

From Eq. (6), by considering that in Eq. (7) in the temperature range of interest one has $T \ll 2\pi T_s$, one can write

$$T_N(x) \propto \frac{(1-x)^2}{T_s^2(x)} e^{4\pi T_s(x)/T_N(x)} \quad (9)$$

that in the assumption of Eq. (8) yields

$$\frac{T_N(x)}{T_N(0)} = \frac{1}{(1-x)^2} \exp \left[2.26 \frac{T_{exch}}{T_N(0)} \left[\frac{T_N(0)}{T_N(x)} (1-x)^2 - 1 \right] \right]. \quad (10)$$

One can note that Eq. (9) predicts a slight decrease of T_N with x , with the initial rate close to 2, for $T_{exch} = 1500$ K and $T_N(0) = 310$ K. On the assumption that Eq. (6) is a satisfactory approximation for La_2CuO_4 , our data for $T_N(x)$ can be used to extract quantitative information on the dependence of ξ_{2D} from Zn doping. In this way we derive the expression

$$\xi_{2D}(x) \simeq \xi_{2D}(0) \frac{(1-4x)^{1/2}}{(1-x)}. \quad (11)$$

In charge-doped La_2CuO_4 , a decrease of the spin stiffness is expected to extend the quantum critical regime in which disorder does not affect the universal scaling behavior in terms of correlation length.³⁶ The small effect of Zn on ξ could be interpreted in an analogous way. Furthermore, ξ and T_s only slightly x dependent are consistent with a spin-wave spectrum in the AF phase practically unaffected by Zn, as we shall see in discussing the NQR relaxation rates for $T < T_N$. On the whole, the behavior of $T_N(x)$ and $\langle \mu_{Cu} \rangle$ appear consistent with the main features of a metallic AF,³¹ taking into account that even in this case the effective Hamiltonian and the spin-wave spectrum are well described³⁷ by a localized $S = \frac{1}{2}$ Heisenberg model, provided that the exchange is assumed to vary with x .

With regard to the temperature dependence of the AF field, it appears that the main features for pure La_2CuO_4 are preserved upon Zn doping, up to $x \simeq 0.08$ (Fig. 6). For $T \ll T_N(x)$, the decrease of the field can be analyzed

in terms of the function

$$\rho = [|\mathbf{h}(x, 0)| - |\mathbf{h}(x, T)|] / |\mathbf{h}(x, 0)| = AT^\alpha, \quad (12)$$

which results from spin-wave excitations.³⁸ For a gapless spectrum in 3D Heisenberg AF's one expects $\alpha = 2$, while in the presence of an energy gap E_g , $\rho \propto \exp[-E_g/kT] T^{3/2}$.

From the data in Fig. 6 it turns out that a function of the form $\rho = AT^\alpha$ is consistent with the results up to $T/T_N(x) \simeq 0.6$, with $A \simeq 10^{-5}$ and $\alpha \simeq 1.9$. These estimates can be compared with the ones obtained³⁹⁻⁴² in other AF cuprates such as $\text{YBa}_2\text{Cu}_3\text{O}_6$: $A \simeq 4.5 \times 10^{-6}$ and $\alpha \simeq 1.94$. Large A values and α close to 2 can be justified⁴¹ by expressing the thermal average of the spin components within a detailed model for the spin-wave spectrum. In our case the behavior of ρ indicates that, in spite of the presence of Zn impurities, La_2CuO_4 is still characterized by spin dynamics typical of 2D $S = \frac{1}{2}$ AF's. Only for $T < 20$ K, where the large error prevents quantitative estimate,^{39,42} could the possible occurrence of low-energy excitations⁴³ be considered. In the high-temperature range the behavior of the AF field obviously departs from the one expected from spin-wave excitations. For T close to $T_N(x)$, no particular modifications could be evidenced in the T dependence of $|\mathbf{h}|$ with respect to undoped La_2CuO_4 and we refer for comments to Ref. 21. A remark is in order in light of a recent derivation for the magnetization in Heisenberg systems based on the decoupling of spin-wave and spin-flip thermal contributions.⁴⁴ Our data for $|\mathbf{h}|$ in the vicinity of the phase transition appear close to the behavior calculated by Serena, Garcia, and Levanyuk⁴⁴ from their effective Ising model approximation.

For strong doping ($x \geq 0.1$), $|\mathbf{h}(x, T)|$ shows anomalies in the low-temperature region. Because of the lack of sufficient resolution we delay an analysis of this aspect to further work. We observe here that these anomalies are consistent with the picture of progressive freezing of extra magnetic moments induced on the Cu orbitals by Zn (see below). For large x , when for $T \rightarrow 0$ the freezing leads to spin-fluctuation frequencies below the linewidth, a modification in the static field at the La site can actually be expected.

Let us now discuss the temperature and doping dependence of the ^{139}La NQR relaxation rates (Fig. 7) in terms of the Cu^{2+} cooperative dynamics and spin excitations. From Eq. (5), by relating the fictitious field at the La site \mathbf{h} to the Cu^{2+} spin operators \mathbf{S} and introducing the collective variables \mathbf{S}_q , a standard procedure^{45,46} allows one to write

$$2W \simeq \frac{\gamma^2}{(2\pi)^2} (\mathbf{h}_{\text{eff}})^2 \frac{kT}{N} \sum_q \chi_q(0) J_q(3\omega_q), \quad (13)$$

where \mathbf{h}_{eff} is an effective field mediated over the Brillouin zone and close to the value $|\mathbf{h}| \simeq 10^3$ G found in La_2CuO_4 at the lowest temperature. It should be noted that in Eq. (13), $kT\chi_q(0) = |\mathbf{S}_q|^2$ and average isotropic static susceptibility $\chi_q(0)$ and spectral density $J_q(\omega)$ are introduced from the dipolar part of the nucleus-electron Hamiltonian,¹¹ which in the correlation functions for the transverse

components of \mathbf{h} also brings in the longitudinal fluctuations of \mathbf{S} .⁴⁵

Referring to Fig. 7, let us first discuss the relaxation rates for $T \geq 100$ K. In the AF phase the relaxation is generally driven by the Raman two-magnon process.^{47,48} In the assumption of a gapless spectrum and for 3D isotropic AF with a single superexchange interaction $J_{\text{exch}} = \omega_e \hbar$, one can write for the two-magnon relaxation process

$$2W \approx \frac{1}{5\pi} \gamma^2 h_{\perp}^2 \frac{1}{\omega_e} \left[\frac{T}{T_{\text{exch}}} \right]^3 \quad (T < T_N), \quad (14)$$

with h_{\perp} the transverse component (with respect to V_{zz}) of the field \mathbf{h} . Equation (14) corresponds to an effective q -integrated spectral density $J_{\text{eff}} \equiv (1/N) \sum_{\mathbf{q}} J_{\mathbf{q}}(\omega \rightarrow 0)$ in Eq. (13) of the form $J_{\text{eff}} \approx (1/\omega_e)(T/T_{\text{exch}})^3$. In the presence of a gap $\hbar\Delta$ in the spin-wave spectrum a further term of the form $(\hbar\Delta/kT) \exp[-\hbar\Delta/kT]$ should be included in Eq. (14), only for $T \leq (\hbar\Delta/k)$. One sees that below T_N , a fast decrease of the La NQR relaxation rate on cooling can be expected. With regard to the absolute value, it should be remarked that if one uses $\omega_e \approx 5 \times 10^{14}$ rad s⁻¹, then from Eq. (14) a value for W orders of magnitude smaller than the experimental one would be derived. Even though a spin-wave spectrum appropriate to 2D La₂CuO₄ is used in the derivation⁴⁹ agreement is still not found, as already observed for ⁶³Cu relaxation.^{43,50} The large discrepancy between the experimental results and the W 's estimated for the spin-wave excitations is most likely due to the presence of a second relaxation mechanism. The nonperfect oxygen stoichiometry, even in nominally pure La₂CuO₄, with a strong contribution to W arising from the diffusion of extra holes,⁵⁰ is the most natural origin for the increase of ¹³⁹La NQR W with respect to the value for magnon-induced relaxation. Recent measurements²¹ in La₂CuO₄ annealed in different conditions, with $2W$ spanning from about 10⁻³ to 1 s⁻¹ at $T \approx 10$ K, support this hypothesis.

In the temperature range $100 < T < T_N$, only a slight dependence of W with a Zn amount is observed (Fig. 7). Due to the topological disorder in the AF interactions related to Zn, some modifications in the spin-wave spectrum can be expected.⁵¹ In particular, propagating spin waves can exist only for wave vector \mathbf{q} larger than ξ^{-1} . Thus, one has regions of magnetization density short range ordered in space which relax with a time scale related to ξ^{-1} . To discuss these effects we can model the spectral density in Eq. (13) in the form

$$J_{\mathbf{q}}(\omega) = \frac{1}{2\pi} \left[\frac{\Gamma_{\text{SF}}}{(\omega - \omega_{\mathbf{q}})^2 + \Gamma_{\text{SF}}^2} + \frac{\Gamma_{\text{SF}}}{(\omega + \omega_{\mathbf{q}})^2 + \Gamma_{\text{SF}}^2} \right], \quad (15)$$

suggested from neutron scattering in disordered 2D AF's.^{52,53} Γ_{SF} heuristically describes the relaxational dynamics associated with the AF disorder and/or with finite-size effects, while $\omega_{\mathbf{q}} = (c_{\text{SW}}^2 \mathbf{q}^2 + \Delta^2)^{1/2}$. By taking into account that in Eq. (13), $\chi_{\mathbf{q}}(0) \approx |S_{\mathbf{q}}|^2$ is only slightly \mathbf{q} and x dependent^{11,15} and thus $kT\chi(\mathbf{q}, 0) \approx S(S+1)/3$, a 2D integration in the Brillouin zone yields $W \propto J_{\text{eff}}$, with

$$J_{\text{eff}}(3\omega_Q \approx 0) \approx \frac{1}{2\Gamma_{\text{SF}}} \left[\frac{\Gamma_{\text{SF}}}{\Gamma_{\text{SW}}} \right]^2 \ln \frac{\Gamma_{\text{SW}}^2 + \Delta^2 + \Gamma_{\text{SF}}^2}{\Gamma_{\text{SF}}^2 + \Delta^2}, \quad (16)$$

where $\Gamma_{\text{SW}} = c_{\text{SW}} \mathbf{q}_m$, with $\mathbf{q}_m \approx \pi/a$ maximum wave vector, is a typical spin-wave frequency. For strong "disorder" in the AF phase the number of modes contributing to the central component [$(\Gamma_{\text{SF}}/\Gamma_{\text{SW}})^2$ in Eq. (16)] increases, $\Gamma_{\text{SF}} \approx \Gamma_{\text{SW}} \approx \omega_e$ and $J_{\text{eff}} \approx \omega_e^{-1}$, as for the paramagnon excitations in the high-temperature limit. In light of Eq. (16), one can conclude that the presence of topological disorder in the AF interactions should increase the relaxation rate. Furthermore, Zn doping is expected to decrease slightly the spin-wave velocity c_{SW} ,³¹ implying a decrease of Γ_{SW} . From Fig. 7, by considering temperature range above about 100 K, it appears that the increase with x is modest. One can conclude that the spin-wave spectrum is substantially unaltered by Zn doping. Recent neutron scattering experiments in the AF phase of YBa₂CuO_{6+x}, where the spin excitation spectrum at $T=100$ K was found practically unaffected by Zn,⁵⁴ corroborate this conclusion.

Let us analyze the most remarkable effect of Zn on the ¹³⁹La NQR relaxation rate, namely, the x and temperature behavior for $T \leq 100$ K (Fig. 7). The maxima in W indicate a relaxation mechanism whose characteristic fluctuation frequency becomes of the order of $3\omega_Q$ at T_m . This mechanism, which is superimposed on the spin-wave background, can be related to the cooperative freezing of local effective magnetic moments μ_e induced by Zn on the Cu orbitals. These moments have been recently detected in YBa₂(Cu_{1-y}Zn_y)O_{6+x} and studied with ⁸⁹Y NMR (Ref. 9) and μ SR (Ref. 10) and cause a spin texture in the AF ordered planar Cu²⁺ arrangement. In particular the μ SR measurements, being in zero external field, prove that the extra magnetic moments are not field induced and then present in the NQR regime also. To account for the relaxation process driven by the fluctuations of μ_e , one can extend the picture of the NQR relaxation due to paramagnetic impurities, in the absence of spin diffusion.⁵⁵ On the assumption of an exponential correlation function for $\mu_e(t)$, with a decay rate Γ_{SF} , one can introduce a site-dependent ¹³⁹La NQR relaxation rate

$$W(r_i) \approx a \gamma^2 h_e^2(r_i) \Gamma_{\text{SF}} / (\Gamma_{\text{SF}}^2 + \omega^2), \quad (17)$$

where $h_e(r_i)$ are the transverse components of the magnetic field created at the i th La nucleus at distance r_i from the effective magnetic moment. In light of Eq. (3) and with the experimental corroboration discussed in Sec. IID one should remember that within the first decade the recovery law at the given nucleus has to be considered exponential. However, the configuration average involved in the recovery of the NQR signal from the whole sample leads to a distribution of site-dependent relaxation rates. Thus a nonexponential recovery results in

$$y(t) = \left\langle \exp \left[-t \sum_j W(r_{ij}) \right] \right\rangle_i = \exp \{ -[tW_e]^{1/2} \} \quad (18)$$

(the summation is on the Zn sites). A similar expression has recently been derived for muon spin depolarization in spin glasses.⁵⁶

It should be remarked that the nonexponential recovery is the consequence of the absence of a fast nuclear spin diffusion process which prevents a common spin temperature also at long times.⁵⁷ Then, by using our Eq. (17) in the expression of Ref. 55, the contribution to the ¹³⁹La NQR effective relaxation rate W_e from μ_e can be written

$$2W_e = \frac{32}{45} \pi^3 \gamma^2 \mu_e^2 N_{\text{Cu}}^2 x^2 \frac{\Gamma_{\text{SF}}}{\Gamma_{\text{SF}}^2 + 9\omega_Q^2} \quad (19)$$

(N_{Cu} is the number of Cu atoms per unit volume).

The peculiar aspects of the relaxation process induced by μ_e are the nonexponential recovery and the x^2 dependence of W_e . As shown in Fig. 2, for $T \simeq T_m$ the recovery is actually given by Eq. (4). The x^2 dependence of W_m is also clearly observed (Fig. 8). A further check can be carried out in terms of the quantitative strength of the process, by using in Eq. (19) the value $\mu_e \simeq 0.36\mu_B$ for Zn impurity and considering W_e at T_m where the maxima occur (namely, for $\Gamma_{\text{SF}} = 3\omega_Q$). One obtains $2W_m \simeq 0.6 \times 10^4 x^2 \text{ s}^{-1}$, of the correct order of magnitude. A possible distribution of Γ_{SF} tends to reduce the maxima in the relaxation rates.

From the data in Fig. 7 one can extract the x dependence of the freezing temperature. One obtains $T_m(x) = a + bx$, with $a = 35 \text{ K}$ and $b = 330 \text{ K}$, at least for $x \geq 0.025$. Below T_m the fluctuation frequencies of μ_e are very slow ($\Gamma_{\text{SF}} \ll \omega_Q$) and then one can think that the line $T_m(x)$ separates a phase of a disordered paramagnet from a spin-glass state, superimposed on the AF ordered matrix (see inset in Fig. 7).

For $T \gg T_m$ one has $W \propto \Gamma_{\text{SF}}^{-1}$ and from the experimental values one can derive the activation energy E_A for the cooperative freezing. Because of the limited temperature range only an approximate evaluation can be given: $E_A \simeq 260 \text{ K} \pm 40 \text{ K}$, almost x independent.

The above findings about the freezing process for μ_e can be compared with the charge localization in Sr-doped La_2CuO_4 . In the case of $\text{La}_{2-x}\text{Sr}_x\text{CuO}_4$, one has extra

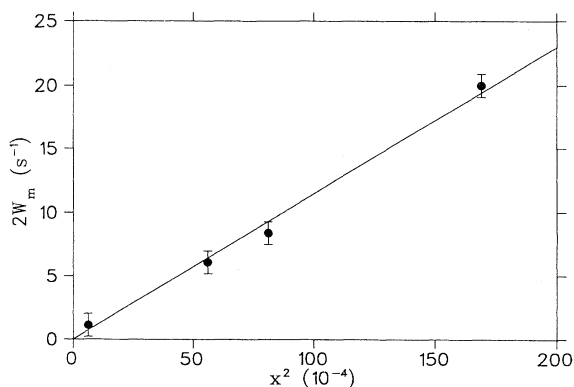


FIG. 8. x dependence of the maxima in the relaxation rates at $T = T_m$, in light of Eq. (19) and for the data shown in Fig. 7. A background contribution of 1 s^{-1} , as present in pure La_2CuO_4 , has been subtracted.

holes hopping in the AF matrix. The holes destroy locally the AF order and cause the relaxation. An expression analogous to Eq. (19) is derived for the relaxation rate, which at the maximum W_m reads⁵⁰

$$2W_h(T = T_m) \simeq 0.13 \gamma^2 a^2 \mu_{\text{Cu}}^2 \frac{c_h}{d_m^3} \frac{1}{\omega_R}, \quad (20)$$

where a is a constant of the order of the unity ($a\mu_{\text{Cu}}$ is the effective magnetic moment originated by the change in the surrounding CuO_2 lattice), d_m is the distance of maximum approach of the holes to the resonant nucleus, c_h the hole concentration, and ω_R the resonance frequency. For ¹³⁹La NQR, assuming d_m as an average distance of the order of $V_c^{1/3}$ (V_c is unit cell volume) and $a = 1$, Eq. (20) becomes

$$2W(T_m) = 0.3 \gamma^2 \mu_{\text{Cu}}^2 \frac{e}{V_c^6} \frac{1}{3\omega_Q}. \quad (21)$$

A comparison with Eq. (19), where $N_{\text{Cu}}^2 = 1/V_c^6$, indicates that a significant difference between the relaxation processes induced by hole and by spin freezing involves the x dependence. A further aspect worth discussing the comparison between $\text{La}_2\text{Cu}_{1-x}\text{Zn}_x\text{O}_4$ and $\text{La}_{2-x}\text{Sr}_x\text{CuO}_4$ is the temperature range below the localization of the extra hole. In $\text{La}_{2-x}\text{Sr}_x\text{CuO}_4$ for $x < 0.02$, the extra holes can localize at $T_{\text{loc}} \simeq 30 \text{ K}$, circulating only along the boundary of four Cu plaquettes.³ The alteration in the underlying spin texture corresponds to a localized magnetic moment, somewhat analogous to the one caused by the Zn impurity. On cooling below T_{loc} the ¹³⁹La NQR relaxation rate passes through a maximum²⁹ which has been attributed to a spin freezing process. For $x < 0.02$, one has²⁹ $T_f(x) \simeq (815 \text{ K})x$. These features have been explained³ in terms of topological excitations and their pair interaction energy. In comparison with Zn-doped La_2CuO_4 , we remark the following. The absolute values of ¹³⁹La NQR W at T_f in $\text{La}_{2-x}\text{Sr}_x\text{CuO}_4$ are larger than the ones at T_m in $\text{La}_2\text{Cu}_{1-x}\text{Zn}_x\text{O}_4$ by a factor around 100 (about $2W_m \propto 2.5 \text{ s}^{-1}$ for $x = 0.025$ in Zn-doped La_2CuO_4 , while $2W_m \simeq 300 \text{ s}^{-1}$ for $x = 0.018$ in $\text{La}_{2-x}\text{Sr}_x\text{CuO}_4$; it should be noted that in Ref. 29 the quantity $R_1 \simeq 23W$ is reported). The x dependence of $W(T_f)$ is difficult to extract but appears to be in between x and x^2 . Therefore, the comparison seems to indicate an effective electron-nucleus interaction for charge localization stronger than the one present upon spin freezing in Zn-doped La_2CuO_4 . Finally, we observed that for Zn-doped La_2CuO_4 , $T_m(x)$ does not extrapolate at zero, in contrast to the case of charge localization in $\text{La}_{2-x}\text{Sr}_x\text{CuO}_4$. This could indicate either a limited number of charge defects or a change of law in the x dependence of T_m for small x . A quantitative comparison of the effects of Zn doping on the spin texture and on the related interaction energy among defects vis-à-vis the correspondent situation for localized charges requires more theoretical and experimental work.

V. SUMMARIZING REMARKS AND CONCLUSIONS

From ¹³⁹La NQR spectra and μ^+ SR it appears that the Néel temperatures and the sublattice magnetization of La₂CuO₄ are affected by Zn doping similarly to what is expected for quantum 2D $S = \frac{1}{2}$ Heisenberg systems. The initial suppression rate for $T_N(x)$ is around 4, while $\langle u(x, T \rightarrow 0) \rangle$ is only slightly sensitive to x , with an initial suppression rate close to 1. If the Néel temperature is related to the in-plane correlation length ξ_{2D} by using a mean-field-type argument and the dilution model for the interplanar interactions, then the results indicate that ξ_{2D} depends on Zn doping in a form close to $\xi_{2D}(x) \approx \xi_{2D}(0)[1 - 2x]$. A moderate effect of randomness and disorder would be consistent with the assumption of a paramagnetic phase in the quantum critical regime, which although appropriate for La₂CuO₄ only for $T \gg T_N$, is expected to be extended at lower temperatures upon doping.

The temperature dependence of the static field in La₂Cu_{1-x}Zn_xO₄ is similar to the one in the pure system up to $x \approx 0.08$. For $T/T_N(x) \leq 0.6$, the temperature decrease of the sublattice magnetization is close to the one of 2D $S = \frac{1}{2}$ Heisenberg AF's, provided that the detailed features of the spin-wave spectrum are taken into account. On approaching $T_N(x)$ the magnetization shows a sudden decrease, as in pure La₂CuO₄, which can be described in terms of a small critical exponent β for the order parameter. This is consistent with an increased role of Ising-type thermal fluctuations decoupled from the spin-wave spectrum. For strong doping ($x \geq 0.1$), the behavior of the field indicates anomalies at low temperatures, similar to the ones observed in Sr-doped La₂CuO₄. Further work is necessary to explore this aspect, due to the lack of resolution related to the marked broadening of the NQR for strong doping. A further complication is related to a kind of microscopic phase separation in Zn-rich and Zn-depleted regions, as it appears from NQR spectra as well as from μ SR, in strongly doped samples.

The NQR relaxation rates indicate that for $T \geq 100$ K the spectrum of the spin-wave excitations is little affected by Zn. In fact, the absolute values and the temperature dependence of relaxation rates depend only slightly on x . The effect of doping in this temperature range is likely reflected in the W from the decrease of the spin stiffness and/or from boundary constraints on the spin-wave propagation in 2D AF islands of reduced size.

Below $T \approx 100$ K a remarkable phenomenon is observed. The relaxation rates show marked maxima W_m at a temperature T_m , with both W_m and T_m x dependent. On the basis of a theoretical picture based on the relaxation process driven by randomly distributed impurities, the peculiar behavior of W has been justified by considering how Zn introduces extra magnetic moments on Cu orbitals, as recently detected from μ SR and Y NMR in YBa₂Cu₃O₇. These magnetic moments form a disordered paramagnet superimposed on the AF matrix. Their progressive freezing, on cooling, induces a spin-glass state when the characteristic fluctuation frequencies becomes of the order of the quadrupole frequencies. In agreement with a relaxation process driven by disordered magnetic impurities, the relaxation rate W_m depends on x^2 . A comparison has been made with the equivalent situation occurring in Sr-doped La₂CuO₄ in the temperature range where for low x the extra hole becomes localized.

ACKNOWLEDGMENTS

Useful discussions with M. Acquarone, H. Alloul, F. Borsa, and R. Gooding are gratefully acknowledged. Thanks are due to M. Bertassi and particularly to F. Raffa for their help in carrying out some measurements and for the elaboration of the data. Finally, we would like to acknowledge the excellent technical assistance by S. Aldrovandi. This work was supported by CNR of Italy in the framework of the "Progetto Finalizzato Tecnologie Superconduttive e Criogeniche" and by INFN (Istituto Nazionale Fisica della Materia).

*On leave from Department of Physics, Hacettepe University, Ankara, Turkey.

¹Proceedings of the International Conference on Material and Mechanisms of Superconductivity—High Temperature Superconductors, Grenoble, 1994, edited by P. Wyder [Physica C **235-240**, (1994)].

²See Johnston *et al.*, Physica C **235-240**, 257 (1994), and references therein.

³R. J. Gooding, N. M. Salem, and A. Mailhot, Phys. Rev. B **49**, 6067 (1994).

⁴A. Chakraborty, A. J. Epstein, M. Jarrel, and E. M. McCarron, Phys. Rev. B **40**, 5296 (1989).

⁵A. R. McGurn, J. Phys. C **12**, 3525 (1979).

⁶D. J. Breed, K. Gilliamse, J. W. Sterkenburg, and A. R. Miedema, J. Appl. Phys. **41**, 1982 (1970); B. J. Dikken, A. F. M. Arts, H. W. De Wijn, W. A. H. M. Vlask, and E. Frikken, Phys. Rev. B **32**, 1267 (1985).

⁷S. W. Cheong, A. S. Cooper, L. W. Rupp, B. Battlog, J. D. Thompson, and Z. Fisk, Phys. Rev. B **44**, 9739 (1991).

⁸See, for instance, K. Umezawa, Physica C **185**, 1159 (1991); L. Cao, L. Zhu, and Z. Cheng, *ibid.* **185**, 815 (1991); P. Carretta *et al.*, *ibid.* **191**, 97 (1992); Bala Krisnan *et al.*, *ibid.* **161**, 9 (1989).

⁹A. V. Mahajan, H. Alloul, G. Collin, and J. F. Marucco, Phys. Rev. Lett. **72**, 3100 (1994).

¹⁰P. Mendels *et al.*, Phys. Rev. B **49**, 10035 (1994).

¹¹See, among others, F. Borsa, M. Corti, T. Rega, and A. Rigamonti, Nuovo Cimento D **11**, 1785 (1989); A. Rigamonti, F. Borsa, M. Corti, T. Rega, and F. Waldner, in *Earlier and Recent Aspects of Superconductivity*, edited by J. C. Bednorz and K. A. Müller (Springer, Berlin, 1990), p. 441; A. Rigamonti, M. Corti, T. Rega, J. Ziolo, and F. Borsa, Physica C **166**, 310 (1990); J. H. Cho, F. Borsa, D. C. Johnston, and D. R. Torgeson, Phys. Rev. B **46**, 3179 (1992).

¹²M. Corti, A. Lascialfari, A. Rigamonti, F. Tabak, F. Licci, and L. Raffo, J. Appl. Phys. **75**, 7143 (1994); M. Corti, A. Rigamonti, F. Tabak, P. Carretta, F. Licci, and L. Raffo, Physica C **235-240**, 1719 (1994).

- ¹³H. Alloul, T. Ohno, H. Casalta, J. F. Marucco, F. Mendels, S. Arabsky, and G. Collins, *Physica C* **171**, 419 (1990).
- ¹⁴H. Alloul, P. Mendels, H. Casalta, J. F. Marucco, and J. Arabsky, *Phys. Rev. Lett.* **67**, 3140 (1991).
- ¹⁵B. Keimer, A. Aharony, A. Auerbach, R. J. Birgenau, A. Cassanho, Y. Endoh, R. W. Erwin, M. A. Kastner, and G. Shirane, *Phys. Rev. B* **46**, 14034 (1992).
- ¹⁶L. Raffo, F. Licci, and A. Migliori, *Phys. Rev. B* **48**, 1192 (1993).
- ¹⁷See S. Rubini *et al.*, *Physica C* **235-240**, 1717 (1994).
- ¹⁸H. Nishihara, H. Yasuoka, T. Shimizu, T. Tsuda, T. Imai, S. Sasaki, S. Kanbe, K. Kishio, K. Kitazawa, and K. Fueki, *J. Phys. Soc. Jpn.* **56**, 4559 (1987).
- ¹⁹Y. Kitaoka, S. Hiramatsu, K. Ishida, T. Kohara, and K. Asayama, *J. Phys. Soc. Jpn.* **56**, 3024 (1987).
- ²⁰T. Rega, *J. Phys. Condens. Matter* **3**, 1871 (1991).
- ²¹I. Watanabe, *J. Phys. Soc. Jpn.* **63**, 1560 (1994).
- ²²D. E. MacLaughlin *et al.*, *Phys. Rev. Lett.* **72**, 760 (1994).
- ²³H. Lutgemeier and M. W. Pieper, *Solid State Commun.* **64**, 267 (1987).
- ²⁴V. A. Borodin *et al.*, *Pis'ma Zh. Eksp. Teor. Fiz.* **52**, 1073 (1990) [*JEPT Lett.* **52**, 468 (1990)].
- ²⁵R. Zysler, D. Fiorani, A. M. Testa, and F. Licci, *Physica C* **235-240**, 1571 (1994).
- ²⁶F. Borsa *et al.*, *Physica C* **235-240**, 1713 (1994).
- ²⁷R. L. Lichti *et al.*, *Physica C* **180**, 356 (1992).
- ²⁸S. T. Ting *et al.*, *Phys. Rev. B* **45**, 11772 (1992).
- ²⁹F. C. Chou *et al.*, *Phys. Rev. Lett.* **71**, 2323 (1993).
- ³⁰Y. Sidid *et al.*, *Physica C* **235-240**, 1591 (1994).
- ³¹M. Acquarone and M. Paiusco, *Physica C* **210**, 373 (1993).
- ³²S. Chakravarty, B. I. Halperin, and D. R. Nelson, *Phys. Rev. Lett.* **60**, 1057 (1988); *Phys. Rev. B* **39**, 2344 (1989).
- ³³P. Hasenfratz and F. Niedermayer, *Phys. Rev. B* **268**, 231 (1991).
- ³⁴M. Greven *et al.*, *Phys. Rev. Lett.* **72**, 1096 (1994).
- ³⁵A. B. Harris and S. Kirkpatrick, *Phys. Rev. B* **16**, 542 (1977).
- ³⁶A. V. Chubukov and S. Sachdev, *Phys. Rev. Lett.* **71**, 169 (1993).
- ³⁷E. Arrigoni and G. C. Strinati, *Phys. Rev. B* **45**, 7816 (1992).
- ³⁸See V. Jaccarino, in *Magnetism II A*, edited by G. T. Rado and H. Suhl (Academic, New York, 1965), p. 322.
- ³⁹C. Bucci *et al.*, *Phys. Rev. B* **48**, 16769 (1993).
- ⁴⁰Y. Iwamoto *et al.*, *J. Phys. Soc. Jpn.* **61**, 441 (1992).
- ⁴¹M. Matsumura *et al.*, *J. Phys. Soc. Jpn.* **62**, 4081 (1993).
- ⁴²A. Lombardi *et al.*, *Physica C* **235-240**, 1651 (1994).
- ⁴³T. Tsuda, T. Ohno, and H. Yasuoka, *J. Phys. Soc. Jpn.* **61**, 2109 (1994).
- ⁴⁴P. A. Serena, N. Garcia, and A. P. Levanyuk, *Phys. Rev. B* **50**, 1008 (1994).
- ⁴⁵For details, see F. Borsa and A. Rigamonti, in *Magnetic Resonance at Phase Transitions*, edited by F. J. Owens, C. P. Poole, and H. A. Farach (Academic, New York, 1979).
- ⁴⁶H. Benner and J. P. Boucher, in *Magnetic Properties of Layered Transition Metal Compounds*, edited by L. J. de Jongh (Kluwer, Dordrecht, 1990), p. 323.
- ⁴⁷T. Moriya, *Prog. Phys.* **16**, 641 (1956).
- ⁴⁸D. Beeman and P. Pincus, *Phys. Rev.* **166**, 359 (1968).
- ⁴⁹S. Chakravarty *et al.*, *Phys. Rev. B* **43**, 2796 (1991).
- ⁵⁰P. Carretta, M. Corti, and A. Rigamonti, *Phys. Rev. B* **48**, 3433 (1993), and references therein.
- ⁵¹O. Scharpf and H. Capelmann, *Z. Phys. B* **86**, 59 (1992).
- ⁵²See T. Freltoft *et al.*, *Phys. Rev. B* **44**, 5046 (1991); S. M. Hayden *et al.*, *Phys. Rev. Lett.* **68**, 1061 (1991); S. M. Hayden *et al.*, 1061 (1992).
- ⁵³J. N. Tranquada *et al.*, *Phys. Rev. Lett.* **64**, 800 (1990), and references therein.
- ⁵⁴P. Bourges *et al.*, *Physica C* **235-240**, 1683 (1994).
- ⁵⁵M. R. MacHenry, B. G. Silbernagel, and J. H. Wernick, *Phys. Rev. B* **5**, 2958 (1972).
- ⁵⁶I. A. Campbell *et al.*, *Phys. Rev. Lett.* **72**, 1291 (1994).
- ⁵⁷See W. E. Blumberg, *Phys. Rev.* **119**, 79 (1960).